CASTRO-ORGAZ, O., and CHANSON, H. (2016). "Minimum Specific Energy and Transcritical Flow in Unsteady Open-Channel Flow. Closure" *Journal of Irrigation and Drainage Engineering*, ASCE, Vol. 142, No. 10, Paper 07016015, 7 pages (DOI: 10.1061/(ASCE)IR.1943-4774.0001076) (ISSN 0733-9437 [Print]; ISSN: 1943-4774 [online]).

# Closure to "Minimum Specific Energy and Transcritical Flow in Unsteady Open Channel Flow"

Oscar Castro-Orgaz and Hubert Chanson

The Authors thank the Discussers for their interest in the original paper, and the comments offered. During the inspection of the Discussers' assertions, it was found that most of them were unsupported by hydraulic analysis. Below a detailed reply to each comment is ellaborated. Bullets are used to differentiate between specific items to be presented.

## General

• First, we clarify, contrary to the Discussers' opening statements, that the paper explored the validity of the steady backwater equation, or gradually-varied flow equation, at the critical depth. The validity of the equation was checked using an unsteady mathematical model, namely the Saint Venant equations, as well as experiments. The backwater equation is obtained simplyfying the differential form of Saint Venant equations to steady state conditions (Montes 1998), namely

$$\frac{\mathrm{d}h}{\mathrm{d}x} = \frac{-\dfrac{\mathrm{d}z_b}{\mathrm{d}x}(x)}{1-\dfrac{q^2}{gh(x)^3}} = \frac{-\dfrac{\mathrm{d}z_b}{\mathrm{d}x}}{1-\mathsf{F}^2} \tag{1}$$

where $h$ is the flow depth, $q$ the discharge and $z_b = z_b(x)$ the bottom profile. Comparison of the solution the backwater equation, and the solution of the integral form of Saint Venant equations, after establishment of a steady state, gave identical results [see Fig. 3 of the original paper]. Comparison of Saint Venant equations with experimental data in Fig. 5b of the original paper gave good results. The analytical solution for the free surface slope at the critical point is

$$\left(\frac{\mathrm{d}h}{\mathrm{d}x}\right)_c = \pm\left(-\frac{h_c}{3}\frac{\partial^2 z_b}{\partial x^2}\right)^{1/2} \tag{2}$$

This equation was compared and verified with the experiments of Wilkinson (1974) in Fig. 4 of the original paper. Using the unsteady flow results from Saint Venant equations, the free surface slope at a section was computed from the finite-difference approximation

$$\frac{\partial h}{\partial x}(x,t) \approx \frac{h_{i+1}(t) - h_{i-1}(t)}{2\Delta x} \tag{3}$$

At the weir crest ($x$ = 0) it was found that the steady-state free surface slope obtained from the unsteady solution of Saint-Venant equation perfectly matched Eq. (2), e.g.

$$\left(\frac{\partial h}{\partial x}(0,t)\right)_{t\to\infty} \to -\left[-\frac{1}{3}\left(\frac{q^2}{g}\right)^{1/3}\frac{\partial^2 z_b}{\partial x^2}\right]_{\text{crest}}^{1/2} \tag{4}$$

This result was also included in Fig. 4 of the original paper. Therefore, the validity of the steady state equations (backwater equation, singular point equation) was verified in the original paper, using both general unsteady mathematical solutions, and laboratory observations. To clearly highlight this fact, the computed free surface profile using Eq. (1), obtained from the Runge-Kutta method, is presented in Fig. 1a [see Fig. 5b of the original paper]. The boundary condition at the weir crest section, $x$ = 0, is $h(0) = h_c = (q^2/g)^{1/3}$. The free surface slope at that section is given by Eq. (2). Subcritical and supercritical profiles were computed from $x$ = 0 in the up- and downstream directions, respectively. Fig. 1a reveals that the accuracy of the computation is good. That Saint Venant theory is mathematically valid at the critical depth means that for the weir flow case investigated in the original paper, mathematical solutions are obtained for arbitray values of $E_{\min}/R$. Consequently, limits to the theory should be set based on experimental observations. This was acomplished in the original paper on the basis of the computation presented in Fig. 5b (current Fig. 1a). The mathematical prediction based on the backwater equation is good if the curvature is small, as in Fig.1a, where $E_{\min}/R$ = 0.253. The experimental verification of Eq. (2) is presented in the current Fig. 1b, based on Fig. 4 of the original paper. This analytical solution is seen to be in excellent agreement with experiments up to $-h_c\, d^2z_b(x)/dx^2 \approx 0.15$, or $E_{\min}/R \approx 3/2\cdot 0.15 = 0.225$. Therefore, the solution of the backwater Eq. (1), including Eq. (2), are in full agreement with the more general solution of Saint Venant equations, and these solutions are verified to be physically good if the curvature is small, e.g. for $E_{\min}/R < 0.25$.

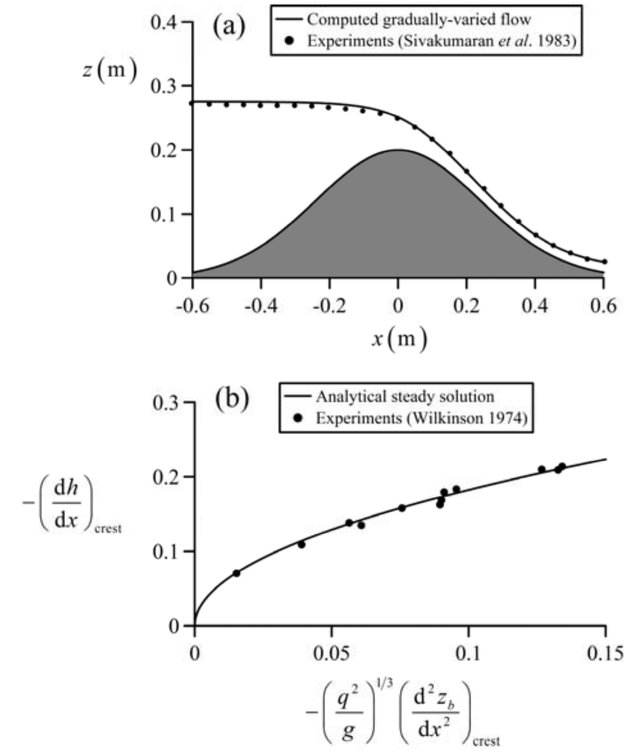


Figure 1. Validity of gradually-varied flow theory and singular point method (a) free surface profile computed applying the singular point method to the backwater equation, for a test case of Sivakumaran *et al.* (1983) with $E_{\min}/R$ = 0.253 and $q$ = 0.0359 m$^2$/s, (b) experimental verification of the free surface slope at a control section computed using the singular point method

• For steady, frictionless flow over a weir, Eq. (1) is equivalent to the differential form of

$$H = z_b + h + \frac{q^2}{2gh^2} = \text{const} \tag{5}$$

It means that based on Eq.(5) smooth mathematical solutions for transcritical flow over a weir are obtained (Fig. 1a). Equation (1) is consistent with the formation of steady singular points, asymptotically, during an unsteady flow computation based on the Saint Venant equations

$$\frac{\partial \mathbf{U}}{\partial t} + \frac{\partial \mathbf{F}}{\partial x} = \mathbf{S} \tag{6}$$

Here **U** is the vector of conserved variables, **F** is the flux vector and **S** the source term vector, given by

$$\mathbf{U} = \begin{pmatrix} h \\ hU \end{pmatrix}; \quad \mathbf{F} = \begin{pmatrix} hU \\ hU^2 + \frac{1}{2}gh^2 \end{pmatrix}; \quad \mathbf{S} = \begin{pmatrix} 0 \\ gh\left(-\frac{\partial z_b}{\partial x} - S_f\right) \end{pmatrix} \tag{7}$$

where $U$ is the depth-averaged velocity. Results in Figs. 3 and 4 of the original paper indicated that both results almost perfectly match, thereby indicating that the unsteady flow over a weir produces a singular point asymptotically in the crest section as the steady state is approached.

• The Discussers used the terminology "Singular Point Theory", which is not adequate. There is not such a theory. What is under debate is the "Singular point Method", as correctly named by the Authors in the original paper and by Chow (1959, pages 237-242), among others. The singular point method is a mathematical technique used to solve indeterminations in ordinary differential equations. Therefore, it is a mathematical method that can be applied to different theories. It is a very common tool in applied mathematics (see e.g. von Kármán 1940) used to model dynamic systems in physics and engineering.

• The normal depth concept is not used in the original paper, given that flow over a weir crest can be considered a potential flow, as verified experimentally (Montes 1998).

• Broad-crested weirs are not considered in the original paper, contrary to what the Discussers suggested. We considered flow over a weir crest, where $z_b(x)$, $\mathrm{d}z_b(x)/\mathrm{d}x$ and $\mathrm{d}^2z_b(x)/\mathrm{d}x^2$ are smooth and continous.

• In their experimental setup, the Discussers found various singular points. To determine the actual flow profile, sub- and supercritical profiles are computed from each singular point. Between each pair of singular points, a supercritical flow profile computed from the singular point upstream, must be ensembled with a subcritical flow profile computed from the singular point downstream, studying the formation of a hydraulic jump. If a jump is formed, both singular points acts as controls. If a jump is not formed, only one singular point will be an active control section, and the profile betwen the two singular points will be fully subcritical or supercritical. We recall that a characteristic feature of a singular point is the possibility of transcritical flow profiles across them, when it acts as a control, and the variety of profile in its vicinity, not crossing it. The number of possible cases is long, and there is no space for a detailed description in this closure paper. We advice the Discussers to consult the work of Iwasa (1958).

## Hydrostatic modelling

• The Discussers asserted that " *there is no reason for both numerator and denominator, each different functions of x and h, going to zero at the same point in (x, h) space*", with reference to the simgular point of Eq. (1). We give mathematical proof as follows. Let us write Eq. (1) in the alternative form

$$\frac{\mathrm{d}z_b}{\mathrm{d}x}+\frac{\mathrm{d}h}{\mathrm{d}x}\left(1-\frac{q^2}{gh^3}\right)=0 \quad (8)$$

Let us define the function of ($x$, $h$) space

$$I\left(x,h\right)=\frac{\mathrm{d}z_b}{\mathrm{d}x}+\frac{\mathrm{d}h}{\mathrm{d}x}\left(1-\mathsf{F}^2\right) \quad (9)$$

Any point of the ($x$, $h$) space that produces the following identity

$$I\left(x,h\right)\equiv 0 \quad (10)$$

is by definition a solution of the ODE given by Eq. (8). Now, let us consider a point $x = x_o$ where $\mathrm{d}z_b(x)/\mathrm{d}x = 0$. Solutions of the ODE at this point must verify, therefore, the identity

$$I\left(x_o,h\right)=\frac{\mathrm{d}h}{\mathrm{d}x}\left(1-\mathsf{F}^2\right)\equiv 0 \quad (11)$$

Based on Eq. (11), the following solutions ($S_1$, $S_2$, $S_3$) are possible at $x = x_o$

$$\begin{aligned}&\frac{\mathrm{d}h}{\mathrm{d}x}=0,\quad \mathsf{F}\neq 1\rightarrow S_1,\\&\frac{\mathrm{d}h}{\mathrm{d}x}\neq 0,\quad \mathsf{F}=1\rightarrow S_2,\\&\frac{\mathrm{d}h}{\mathrm{d}x}=0,\quad \mathsf{F}=1\rightarrow S_3.\end{aligned} \quad (12)$$

The 3 solutions given in Eqs. (12) are mathematically possible, but the physical implication of each one is unclear. To depict physically what each mathematical stament in Eq. (12) indicates, let us differentiate Eq. (8) with respect to $x$, to get

$$\frac{\mathrm{d}^2 z_b}{\mathrm{d}x^2}+\frac{\mathrm{d}^2 h}{\mathrm{d}x^2}\left(1-\frac{q^2}{gh^3}\right)+\left(\frac{\mathrm{d}h}{\mathrm{d}x}\right)^2\frac{3q^2}{gh^4}=0 \tag{13}$$

There is nothing assumed to get Eq. (13), just a differential of Eq. (8) was determined. Now, conditions given by each solution ($S_1$, $S_2$, $S_3$) in Eqs. (12) are complemented with the application of Eq. (13) to yield

$$\begin{aligned}
&S_1 \Rightarrow \frac{\mathrm{d}h}{\mathrm{d}x}=0, \quad \mathsf{F}\neq 1, \quad \frac{\mathrm{d}^2 z_b}{\mathrm{d}x^2}+\frac{\mathrm{d}^2 h}{\mathrm{d}x^2}\left(1-\frac{q^2}{gh^3}\right)=0\\
&S_2 \Rightarrow \frac{\mathrm{d}h}{\mathrm{d}x}\neq 0, \quad \mathsf{F}=1, \quad \frac{\mathrm{d}^2 z_b}{\mathrm{d}x^2}+\left(\frac{\mathrm{d}h}{\mathrm{d}x}\right)^2\frac{3q^2}{gh^4}=0\\
&S_3 \Rightarrow \frac{\mathrm{d}h}{\mathrm{d}x}=0, \quad \mathsf{F}=1, \quad \frac{\mathrm{d}^2 z_b}{\mathrm{d}x^2}=0
\end{aligned} \tag{14}$$

Based on the mathematical results in Eqs. (14):

(i) Solution $S_1$ implies a subcritical ($\mathsf{F} < 1$), or supercritical ($\mathsf{F} > 1$), flow at the weir crest [$\mathrm{d}z_b(x)/\mathrm{d}x = 0$], with zero free surface slope. This is the well-known case of a whole subcritical, or supercritical profile, over a hump [see e.g. Jain (2001), page 98].

(ii) Solution $S_2$ implies a critical flow ($\mathsf{F} = 1$) at the weir crest [$\mathrm{d}z_b(x)/\mathrm{d}x = 0$], with the free surface slope given by Eq. (2). To get a physical solution, the condition $\mathrm{d}^2 z_b(x)/\mathrm{d}x^2 < 0$ is required, that is, a critical flow section is formed only in weir flow (convex bottom profile).

(iii) Solution $S_3$ implies a critical flow ($\mathsf{F} = 1$) with $\mathrm{d}z_b(x)/\mathrm{d}x = 0$ and $\mathrm{d}^2 z_b(x)/\mathrm{d}x^2 = 0$. This is the theoretical case of critical, frictionless flow over a horizontal bottom.

The present development is a generalization of a mathematical development by Henderson (1966, pages 40-42). Solution $S_2$ is a general mathematical solution of Eq. (8), and, thus of Eq. (1). Therefore, there is not fortuitous occurence of $\mathrm{d}z_b(x)/\mathrm{d}x = 0$ and $\mathsf{F} = 1$. The critical depth, with finite free surface slope, is one of the possibles solutions of the backwater equation. Inclusion of the friction slope is simple [see e.g. Hager (2010), pages 142-149)], and it is not repeated here.

• Shock capturing finite volume solutions using the Godunov upwind method assisted by robust Riemann solvers, as used in the original paper, yields accurate solutions of shallow-water flows (Toro 2002). The integral form of Eq. (6) over a control volume is (Toro 2002)

$$\int_{\Omega} \frac{\partial \mathbf{U}}{\partial t} \mathrm{d}\Omega + \int_{A} \mathbf{n} \bullet \mathbf{F} \mathrm{d}A = \int_{\Omega} \mathbf{S} \mathrm{d}\Omega \qquad (15)$$

where Ω is the control volume, $A$ the cell boundary area and **n** the outward unit vector normal to $A$. Equation (15) was solved in the original paper using a high-resolution finite volume scheme, where details of the numerical scheme are extensively described. An important aspect that should be clearly understood is that that the integral Eq. (15) is able to describe both continous and discontinous solutions for $\mathbf{U}(x, t)$, without any specific treatment as the flow crosses the critical depth. In the weir flow simulations presented in the original paper, the smooth solution at the weir crest was a mathematical result, found to be in perfect agreement with the singular point method applied to Eq. (1). In weir flow, steady transcritical solutions from $\mathsf{F} <1$ to $\mathsf{F} > 1$ with $dh/dx \rightarrow \infty$ are not possible. However, these are possible in unsteady flow during the propagation of a shock wave [see Fig. 6 of the original paper]. In contrast, steady transcritical solutions from $\mathsf{F} >1$ to $\mathsf{F} < 1$ with $dh/dx \rightarrow \infty$ are possible in the form of a hydraulic jump. All these cases of transcritical flow can be obtained from Eq. (15) without any specific treatment, using a high-resolution Godunov-type numerical scheme.

• The discussers asserted that "*To describe general problems of transitional fow it is necessary to use, at least, Boussinesq equations*". The Saint Venant equations provide very accurate solutions for some transitional flows. To demonstrate that, we have selected two extreme transcritical test cases, widely used in open channel flows (e.g. Khan and Lai 2014, pages 65-69). In Fig. 2, a dam break wave in a dry, rectangular, horizontal flume is considered. The flume is 0.093 m in width, 0.08 m in height, and 20 m in length. The dam was located at coordinate $x$ = 10 m, and the removal was considered instantaneous. The tailwater portion of the flume was initially dry, and the water depth in the dam 0.074 m. Experimental measurements conducted by Schoklitsch (1917) for two times after removal of the dam, namely $t$ = 3.4s and $t$ = 9.4 s, are plotted in Fig. 2a. The flow was modelled using Eq. (15) and the numerical scheme of the original paper, introducing Manning's equation with $n = 0.009$ s/m$^{1/3}$ (Khan and Lai 2014). The effect of the friction slope was introduced implicitly in the numerical model to increasy stability near the wet-dry front. A positivity preserving computational algorithm was coded for the wet-dry front treatment (Khan and Lai 2014). As demonstrated in Fig. 2a, Saint Venant equation can model transcritical open channel flow with great accuracy. In Fig. 2b, we plotted the computed free surface profile at $t$ = 9.4, with indication of the position of the critical flow section, where $\mathsf{F} = U/(gh)^{1/2} = 1$. It can be observed that it is not located at the dam axis. Computations for ideal fluid flow ($S_f$ = 0) yields a result identical to the parabolic, analytical solution by Ritter (Montes 1998)

$$x = x_{\text{dam}} + t\left[3\left(gh\right)^{1/2} - 2\left(gh_o\right)^{1/2}\right] \tag{16}$$

where $h_o$ is the upstream water depth ( = 0.074 m) and the dam coordinate $x_{\text{dam}}$ = 10 m. For Ritter's solution, the flow is exactly critical at the dam axis [see e.g. Jain (2001), page 215]. Therefore, the displacement of the critical point due to friction is seen to be small, and the main effect is confined to the shape of the front. Resort to Boussinesq equations in this case is not needed, therefore.

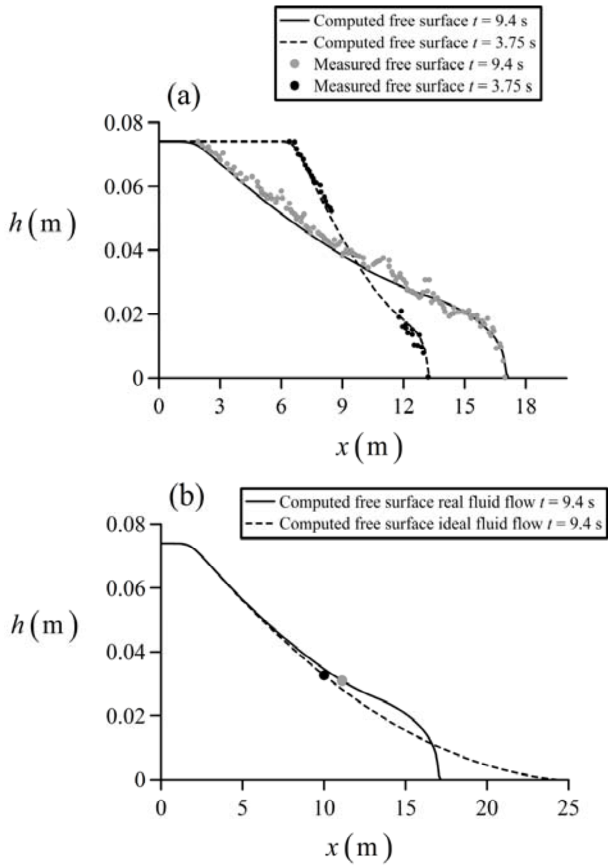

Figure 2. Validity of Saint Venant equations for transcritical flow in a dry-bed dam break wave (a) Comparison of computed and measured (Schoklitsch 1917) instantaneous free surface profiles (b) Comparison of ideal and real fluid flow solutions at $t$ = 9.4 s, and position of critical points (•, •)

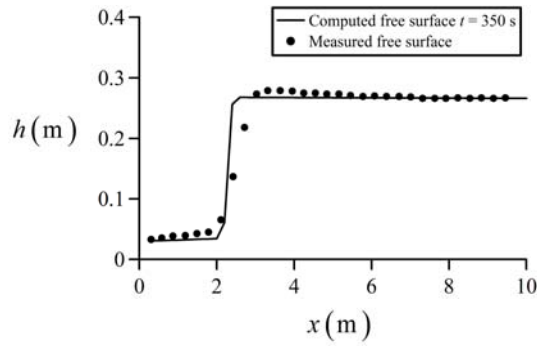


Figure 3. Validity of Saint Venant equations for transcritical flow in a hydraulic jump : Comparison of computed and measured (Gharangik and Chaudhry 1991) steady free surface profiles

A second test of Saint Venant equations for transcritical flow is presented in Fig. 3, where a hydraulic jump measured by Gharangik and Chaudhry (1991) is included. The channel is 14 m long, horizontal, and 0.46 m wide. The Manning's roughness coefficient is $n$ = 0.008 s/m$^{1/3}$ (Khan and Lai 2014). The upstream boundary conditions for the supecritical flow are a water depth of 0.031 m, with a discharge of 0.118 m$^2$/s. At the downstream, subcritical section, only one boundary condition is set, namely the experimentally measured water depth of 0.265 m. The initial free surface profile in the numerical model was taken as a static water layer of 0.031 m. The tailwater level was gradually increased from 0.031 m to 0.265 m in 50s in the numerical model. Computational results obtained at $t$ = 350 s, once a steady-state was reached, are displayed in Fig. 3. It can be seen that Saint Venant equations produce a good transcritical flow simulation, and resort to Boussinesq equations in this test case is not needed.

## Non-hydrostatic modelling

• The Discussers presented in their Fig. 1 experiments for flow over a broad-crested weir, and a simulation unexplained. The lack of any detail in the discussion stating what equation was solved, and the fact that reference to unpublished results was done, made impossible to elaborate a comment on this test and the Discussers' theoretical results. They made reference to a "finite slope" Boussinesq theory, which could not be precisely understood by the Authors what the Disscussers means with that. They also made reference to the Boussinesq theory by Matthew (1991), used by Castro-Orgaz and Hager (2009). Below, we elaborate a detailed reply to explain Boussinesq theory for flows where the bottom slope is finite.

• We resort to the problem of flows from a horizontal to a steep slope. Figure 4 considers one test by Hasumi (1931) for a slope transition composed by a horizontal reach followed by a circular-shaped transition profile of $R$ = 0.1 m that finishes in a steep slope reach of 45º inclination. The discharge is 0.987 $m^2$/s ($h_c$ = 0.10 m). The measured free surface and piezometric bottom pressure head are plotted in the figure. The flow in open channel transitions, including a slope break, can be approximately modeled with the equations of an inviscid and irrotational flow (Montes 1998). The flow problem presented in Fig. 4 was modelled using the Laplacian for $z$ as a function of the pair of variables ($\psi$, $x$)

$$\frac{\partial^2 z}{\partial x^2}\left(\frac{\partial z}{\partial \psi}\right)^2+\frac{\partial^2 z}{\partial \psi^2}\left[1+\left(\frac{\partial z}{\partial x}\right)^2\right]-2\frac{\partial^2 z}{\partial x\partial \psi}\frac{\partial z}{\partial x}\frac{\partial z}{\partial \psi}=0 \qquad (17)$$

where $\psi$ is the stream function. The numerical model developed by Montes (1994) was applied, that is not further described here, therefore. The up- and downstream boundary sections were located at $x/h_c$ = ±3. Twenty streamlines were used to model this flow, and the energy level on the horizontal reach was set to $H/h_c$ = 1.5. The 2D computational results displayed in Fig. 4 show that the ideal fluid flow computation in the slope break problem produces good results. The potential flow approximation is shown, therefore, to be an acceptable approximation.

• To avoid the solution of the full 2D problem, as described above, approximate 1D models for potential flow are desirable. Matthew (1991) developed an approximate Boussinesq theory, where the extended energy equation reads

$$H=z_b+h+\frac{q^2}{2gh^2}\left(1+\frac{2hh_{xx}-h_x^2}{3}+hz_{bxx}+z_{bx}^2\right)=\text{const} \qquad (18)$$

where $h_x = \mathrm{d}h/\mathrm{d}x$, $h_{xx} = \mathrm{d}^2h/\mathrm{d}x^2$, $z_{bx} = \mathrm{d}z_b/\mathrm{d}x$ and $z_{bxx} = \mathrm{d}^2z_b/\mathrm{d}x^2$. The bottom pressure head of Matthew's theory is (Castro-Orgaz and Hager 2009)

$$\frac{p_b}{\gamma} = h + \frac{q^2}{2gh^2}\left(2hz_{bxx} + hh_{xx} - h_x^2 - 2z_{bx}h_x\right) \tag{19}$$

Based on Eqs. (18) and (19), the following observations are made: (i) The theory consider the effect of the curvature of the free surface and the bottom, accounted for by the inclusion of $h_{xx} = \mathrm{d}^2h/\mathrm{d}x^2$ and $z_{bxx} = \mathrm{d}^2z_b/\mathrm{d}x^2$; (i) The theory consider the effect of the slope of the free surface and the bottom, accounted for by the inclusion of $h_x = \mathrm{d}h/\mathrm{d}x$ and $z_{bx} = \mathrm{d}z_b/\mathrm{d}x$. The values of these slopes and curvatures are not necessarily small ones. Therefore, Matthew (1991) theory, used by Castro-Orgaz and Hager (2009), is an approximate potential flow model that includes the effects of finite curvatures and slopes. Friction is not included, however. This limit the application of Matthew's theory to a computational domain where the energy-slope can be taken horizontally, as done by Montes (1994) and Castro-Orgaz and Hager (2009). Results of Castro-Orgaz and Hager (2009) solving Eq. (18) were in good agreement with Eq. (17), and with experimental observations.

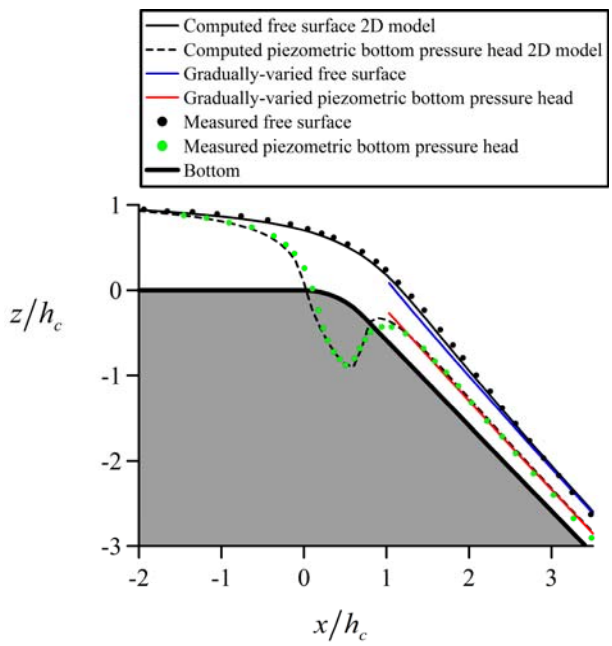


Figure 4. Slope break problem: Comparison of 2D potential flow solution, experimental data (Hasumi 1931), and 1D, potential, gradually-varied flow solution

• Castro-Orgaz and Hager (2009) analyzed the limits of the singular point theory for a slope break. They applied this method to Eq. (1) for slope breaks involving highly curved flows, and concluded that a model based on Eq. (1) can not be applied where the curvature is strong, e.g. in the vicinity of the slope break. This is in full agreement with the original paper, where it was demonstrated that the singular point method applied to Eq. (1) produces good results where the curvature is weak, e.g., see Fig. 1a. Both works are, therefore, in full agreement.

• Castro-Orgaz (2009) found that, despite Eq. (1) can not be applied at the crest zone, given the highly-curved flow, it is a good approximation in the downstream slope for $x/h_c > 1$. Consider for illustrative purposes flows away from the crest, where streamline curvature effects can be neglected. The flow is gradually-varied, meaning that the variation of $h$ with $x$ is small (an hypothesis confirmed by the experimental results plotted in Fig. 4). For these flows, it can be assumned that $h_x^2 \approx h_{xx} \approx 0$. Further, on the slope, the bed is flat, resulting $z_{bxx} = 0$. On this slope, however, the term $z_{bx}$ is finite, and equal to unity in this case. Therefore, despite $h_x$ will be small, the product ($h_x \cdot z_{bx}$) remains finite. Therefore, Eqs. (18) and (19) for gradually-varied, 1D potential flow on a finite slope reads

$$H = z_b + h + \frac{q^2}{2gh^2}\left(1 + z_{bx}^2\right) \tag{20}$$

$$\frac{p_b}{\gamma} = h - \frac{q^2}{2gh^2}\left(2 z_{bx} h_x\right) \tag{21}$$

Castro-Orgaz and Hager (2009) differentiated Eq. (20), producing for large F the ODE

$$\frac{\mathrm{d}h}{\mathrm{d}x} = \frac{z_{bx}}{\frac{q^2}{gh^3}\left(1 + z_{bx}^2\right)} \tag{22}$$

For the horizontal slope reach, the solution of Eq. (22) involving critical flow is solution $S_3$ in Eq. (12). Therefore, the theoretical flow profile is a horizontal line composed of an infinite number of critical points (Castro-Orgaz and Hager 2009). Taking as boundary condition the critical point at the beginning of the slope break, the analytical solution of Eq. (22) for a finite slope is (Castro-Orgaz and Hager 2009)

$$\frac{h}{h_c}=\left(1-\frac{2z_{bx}}{1+z_{bx}^2}\frac{x}{h_c}\right)^{-1/2} \tag{23}$$

Inserting Eq. (22) into Eq. (21) the bottom pressure head is

$$\frac{p_b}{\gamma}=h-\frac{q^2}{2gh^2}\left(2z_{bx}h_x\right)=h\left(1-\frac{z_{bx}^2}{1+z_{bx}^2}\right)=\frac{h}{1+z_{bx}^2} \tag{24}$$

Equation (24) is the "finite slope" approximation for gradually-varied flows, to which the Discussers made reference quoting Fenton (2014). Therefore, based on potential, gradually-varied flow, finite slopes are accounted for both in free surface and bottom pressure head computations. The results of the computations based on Eqs. (23) and (24) are plotted in Fig. 4, for $x/h_c > 1$, as recommended by Castro-Orgaz and Hager (2009). It can be observed that the results are in excellent agreement with experiments, and with the 2D numerical solution.

• If application of a Boussinesq model with friction is found to be necessary, resort to the development by Khan and Steffler (1996) can be made. The Boussinesq version of their theory, for steady flow, reads

$$\frac{\mathrm{d}}{\mathrm{d}x}\left(U^2h+\frac{h}{2}\frac{p_b}{\rho}\right)=-\frac{p_b}{\rho}\frac{\partial z_b}{\partial x}-\frac{\tau_b}{\rho} \tag{25}$$

$$p_b=\rho gh+\rho\frac{U^2}{2}\left(hh_{xx}-h_x^2-2h_xz_{bx}+2hz_{bxx}\right)+\tau_b\frac{\partial z_b}{\partial x} \tag{26}$$

where $\tau_b$ is the bed shear stress. Equations (25) and (26) can be coupled to produce an ODE.

• To show the general applicability of the singular point method, at the time that it is further demonstrated that Boussinesq equations are not the only model that can produce good transcritical flow simulations, we consider here Dressler (1978) theory fow flow over curved beds. For steady flow, the theory gives the following ODE (Sivakumaran and Yevjevich 1987), after re-arrangement,

$$\frac{\mathrm{d}N}{\mathrm{d}\xi}=\frac{-\sin\theta_b\left(1-\kappa_bN\right)-\dfrac{q^2}{g}\kappa_b\dfrac{\mathrm{d}\kappa_b}{\mathrm{d}\xi}\dfrac{\ln\left(1-\kappa_bN\right)+\kappa_bN}{\left[\left(1-\kappa_bN\right)\ln\left(1-\kappa_bN\right)\right]^3}}{\cos\theta_b+\dfrac{q^2}{g}\kappa_b^3\dfrac{\ln\left(1-\kappa_bN\right)+1}{\left[\left(1-\kappa_bN\right)\ln\left(1-\kappa_bN\right)\right]^3}}=\frac{\Phi_1\left(N,\xi\right)}{\Phi_2\left(N,\xi\right)} \tag{27}$$

Here $\xi$ is the bottom-fitted coordinate, $\kappa_b = \kappa_b(\xi)$ the curvature of the bottom profile, $\theta_b$ is the local inclination angle of the bottom profile, $z_b(\xi)$ with the horizontal plane, and the distance from the channel bottom to the free surface is $N$, measured orthogonally outward from the bottom curve. Using the same mathematical development presented with Eqs. (8)-(14), it can be demonstrated that at a weir crest the flow is critical, and Eq. (27) indeterminate. The critical depth is computed setting to zero the denominator of Eq. (27) (Dressler 1978)

$$\Phi_2\left(N_c,\xi\right)=\cos\theta_b+\frac{q^2}{g}\kappa_b^3\frac{\ln\left(1-\kappa_b N_c\right)+1}{\left[\left(1-\kappa_b N_c\right)\ln\left(1-\kappa_b N_c\right)\right]^3}=0 \qquad (28)$$

The solution of the non-linear Eq. (28) by the Newton-Raphson method gave the crest flow depth. Equation (27) was then integrated using the Runge-Kutta method in the up- and downstream directions, starting at the crest. The free surface slope at the crest was found to be, after removal of the indetermination at the weir crest ($c$),

$$\left(\frac{\mathrm{d}N}{\mathrm{d}\xi}\right)_c=-\frac{\left(\frac{\partial\Phi_1}{\partial\xi}\right)_c^{1/2}}{\left(\frac{\partial\Phi_2}{\partial N}\right)_c^{1/2}} \qquad (29)$$

where

$$\left(\frac{\partial\Phi_1}{\partial\xi}\right)_c=-\kappa_b\left(1-\kappa_b N_c\right) \qquad (30)$$

$$\left(\frac{\partial\Phi_2}{\partial N}\right)_c=3\frac{q^2\kappa_b^4}{g}\frac{\left[\ln\left(1-\kappa_b N_c\right)+(5/6)\right]^2+(11/36)}{\left[\left(1-\kappa_b N_c\right)\ln\left(1-\kappa_b N_c\right)\right]^4} \qquad (31)$$

Figure 5a displays the experimental data of Sivakumaran *et al*. (1983) for a symmetrical hump of shape $z_b$ = 20exp[−0.5($x$/24)$^2$] (cm). The unit discharge is 0.11197 m$^2$/s ($h_c$ = 0.1085 m). Computational results are displayed in Fig. 5a, showing good agreement with experimental measurements. The bottom pressure profile $p_b$ was computed from (Dressler 1978)

$$p_b=\rho g N\cos\theta_b+\rho\frac{q^2\kappa_b^2}{2\left[\ln\left(1-\kappa_b N\right)\right]^2}\left[\frac{1}{\left(1-\kappa_b N\right)^2}-1\right] \qquad (32)$$

showing again good agreement with observations in Fig. 5a. These results demonstrate that the singular point method is a mathematical technique that can be applied to different theories, and that transcritical flow problems can also be tackled with other approximations different from Boussinesq equations. Equation (27) was alternatively solved in Fig. 5b taking as starting point the experimentally measured water depth upstream of the hump. Computational results of Fig. 5b reveals that a subcritical flow profile along the entire hump is formed, as found by Sivakumaran *et al*. (1983). A supercritical flow profile can also be determined. This solution was forced by the upstream experimental water depth, which is not permitting the flow to pass across the critical depth.

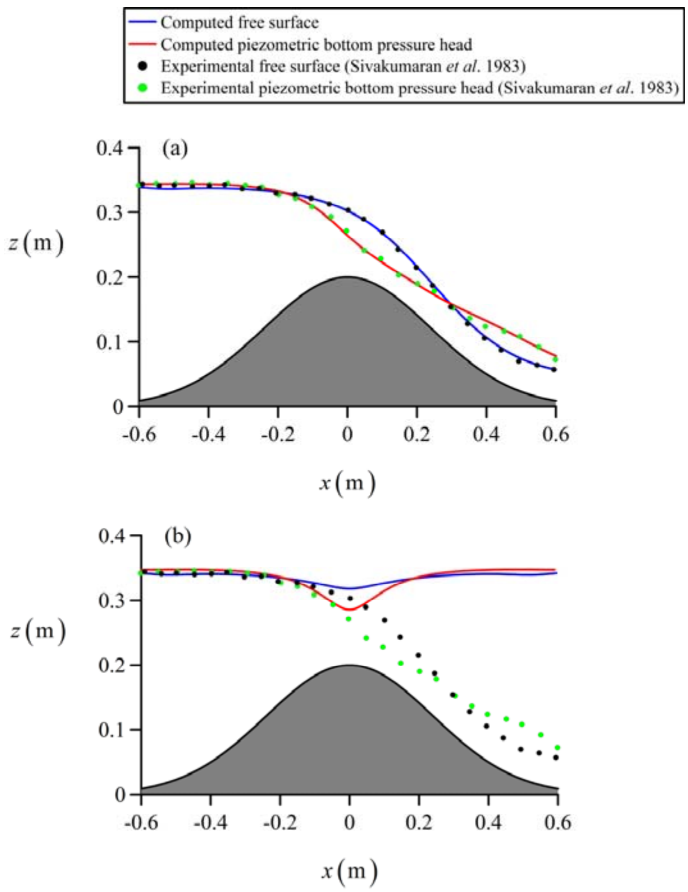


Figure 5. Flow over a hump (a) application of the singular point method to compute transcritical flow using Dressler theory. Simulations are conducted without using any experimental measurement (b) solution of Dressler theory based on the upstream experimental measurement

## Concluding remarks and recommendation

• The singular point method is a useful tool, to be used when needed. As to which model should be proposed to compute transcritical flows, common sense dictates the path to follow. Saint Venant equations are a good model in most cases, like for the computation of the flood inundation area in river flows. If the computation of bed pressures is the main concern, then resort to Boussinesq equations is needed, e.g., for the determination of cavitation risk in a dam spillway crest. Between these two extremes are intermediate options, like use of Dressler theory.

• Since the pioneering work of Bélanger (1828), a number of scholars added to the general body of knowledge today at our hands in the field of open channel hydraulics. We suggest modellers and researches to keep in mind all these computational tools, including the singular point method, to continue advances in this fascinating field of research.

## References

Bélanger, J.B. (1828). Essai sur la solution numérique de quelques problèmes relatifs au mouvement permanent des eaux courantes. Carilian-Goeury, Paris [in French]. (On the numerical solution of some steady water flow problems)

Castro-Orgaz, O., Hager, W.H. (2009). Curved streamline transitional flow from mild to steep slopes. J. Hydr. Res. 47(5), 574-584.

Chow, V.T. (1959). Open channel hydraulics. McGraw-Hill, New York.

Dressler, R.F. (1978). New nonlinear shallow flow equations with curvature. J. Hydr. Res. 16(3), 205-222.

Gharangik, A., Chaudhry, M. (1991). Numerical simulation of hydraulic jump. J. Hydr.. Eng. 117(9), 1195-1211.

Hager, W.H. (2010). Wastewater hydraulics: Theory and practice. Springer, Berlin.

Hasumi, M. (1931). Untersuchungen über die Verteilung der hydrostatischen Drücke an Wehrkronen und -Rücken von Überfallwehren infolge des abstürzenden Wassers. Journal. Dep. Agriculture, Kyushu Imperial University, 3(4), 1-97 [in German].

Henderson, F.M. (1966). Open channel flow. MacMillan, New York.

Iwasa, Y. (1958). Hydraulic significance of transitional behaviours of flows in channel transitions and controls. Memoires of the Faculty of Engineerig, Kyoto University, 20(4), 237-276.

Jain, S.C. (2001). Open channel flow. John Wiley & Sons, New York.

Khan, A.A., Steffler, P.M. (1996). Vertically averaged and moment equations model for flow over curved beds. J. Hydr. Engng. 122(1), 3-9.

Khan, A.A., Lai, W. (2014). Modelling shallow water flows using the discontinuous Galerkin method. CRC Press, Taylor and Francis, London.

Matthew, G.D. (1991). Higher order one-dimensional equations of potential flow in open channels. Proc. ICE 91(3), 187-201.

Montes, J.S. (1994). Potential flow solution to the 2D transition from mild to steep slope. J. Hydr. Engng. 120(5), 601-621.

Montes, J.S. (1998). Hydraulics of open channel flow. ASCE Press, Reston VA.

Schoklitsch, A. (1917). Über dambruchwellen. Kaiserliche Akademie der Wissenschaften, Wien, Mathematisch-Naturwissenschaftliche Klasse, Sitzungberichte IIa, 126,1489–1514 (in German).

Sivakumaran, N.S., Tingsanchali, T. Hosking, R.J. (1983). Steady shallow flow over curved beds. J. Fluid Mech. 128, 469-487.

Sivakumaran, N.S., Yevjevich, V. (1987). Experimental verification of the Dressler curved-flow equations. J. Hydr. Res. 25(3), 373-391.

Toro, E.F. (2002). Shock-capturing methods for free-surface shallow flows. Wiley, New York.

von Kármán, T., Biot, M.A. (1940). Mathematical methods in engineering: an introduction to mathematical treatment of engineering problems. McGraw-Hill, New York.

Wilkinson, D.L. (1974). Free surface slopes at controls in channel flow. J. Hydr. Div., ASCE, 100(8), 1107-1117.

## LIST OF FIGURES